Click to view poster presentation

[EA]Novel Workflow in Modeling Cycles of a Complex Carbonate Reservoirs, Coupling Sequence Stratigraphy and Geostatistics Techniques*

Andi A. B. Salahuddin[1], Reem Al Ali[1], Karem Khan[1], Khaled E. Al Hammadi[1], and Nidhal M. Aljneibi[1]

Search and Discovery Article #42556 (2020)**
Posted October 12, 2020

*Adapted from extended abstract based on poster presentation given at 2020 Geosciences Technology Workshop, 3rd Edition Carbonate Reservoirs of the Middle East, Abu Dhabi, UAE, January 28-29, 2020
**Datapages © 2020. Serial rights given by author. For all other rights contact author directly. DOI:10.1306/42556Salahuddin2020

[1]Abu Dhabi National Oil Company (ADNOC) Onshore, Abu Dhabi, United Arab Emirates (asalahuddin@adnoc.ae)

Abstract

The carbonate reservoir lithofacies discussed in this paper contains heterogeneous pore types and properties. The main difficulty in predicting the flow behavior in such reservoir is related to the heterogeneity, which in turn, would complicate production forecast, field development, and economic evaluation. Modeling discrete properties such as lithofacies presents challenging issues. The geometric anisotropy and petrophysical properties of the individual lithofacies are different and as such, they need to be captured properly. Therefore, an appropriate lithofacies modeling algorithm is a key to build a robust model that represents subsurface heterogeneity which, in turn, is fundamental for realistic simulation forecasts.

Lithofacies geometry and properties studies must form a fundamental basis for characterizing and modeling HRSS framework and lithofacies architecture variability through the reservoir. Combined with wireline-log data, they provide a basis for defining both reservoir framework and rock attribute distributions. In this paper, we present a novel technique for stochastically modeling equiprobable multirealizations of lithofacies and properties distribution by integrating high resolution sequence stratigraphy (HRSS) zonation, depositional environment, and diagenesis trend in combination with geostatistics, dynamic data, and basin-scale geological understanding to represent the subsurface complexity, to generate a holistic reservoirs characterization, and to build reliable static and dynamic models.

The reservoir consists of lagoonal packstone-rudstone, grain rich ooid-peloid shoal, and rudstone-boundstone mid-ramp. The shoal deposits exhibit the best permeability and oil saturation and it consists of discontinuous lithofacies body that depicts locally excellent porosity and permeability characteristics. Complex lithofacies geometries and transitions, both vertically and laterally between the mound and discontinuous grain-rich ooid-peloid shoal lithofacies together with the continuous and sequential lagoonal and mid-ramp lithofacies do not allow single lithofacies model algorithm to simulate these sorts of lithofacies assemblage. Hence a new holistic approach was implemented, a combination of Object Based (OB) algorithm and Truncated Gaussian Simulation (TGS) algorithm to handle the complex lithofacies transition. This enables generating multiple realistic field wide lithofacies distribution and relationship which aligns with data trend, subsurface analog in the nearby

fields, as well as that is from the outcrop exposure. The established lithofacies distribution within HRSS framework was then used to constrain field-wide properties and diagenetic trend and distribution in the reservoir.

This new approach has recently been successfully implemented in the studied field. The resulted geostatistical model was able to explain pressure depletion and production rate as shown in historical production data of the field. The resulting dynamic model will hence provide reliable production forecast and reservoirs development plan which will eventually allow accomplishing the mandate recovery target.

Introduction

The purpose of this paper is to discuss the process of stochastic reservoir modeling and to illustrate the advantages of using a sequence stratigraphic framework in 3-D modeling. Three-dimensional reservoir modeling results in an improved geologic understanding and allows for immediate model updates as new data are acquired. The main difficulties in predicting the flow behavior in complex carbonate reservoirs is related to the heterogeneity which in turn would complicate field development planning. Carbonate sedimentary lithofacies and their related reservoir heterogeneities can be modeled with geostatistical approaches. However, such model needs to consider diagenetic event because the original petrophysical properties were later altered by single or multiple diagenetic events can. The objective of the methodology discussed in this paper is to build a fine grid static geological model which reproduces both the sedimentary lithofacies and the diagenetic trends interpreted from log, core, well tests, and basin scale geological understanding.

Modeling discrete properties such as geological lithofacies presents more challenging issues. The geometric anisotropy and petrophysical properties of the individual lithofacies in the individual depositional systems are different and as such they need to be captured in the geological model for accurate monitoring of reservoir production performance. Therefore, a proper lithofacies modeling algorithm is a key to build a robust model that represents subsurface heterogeneity which is fundamental for realistic simulation forecasts.

Rock properties are keys to production prediction, field development, and economic evaluation. Thus, the construction of reservoir geocellular model from pore to field scale for flow simulation requires the integration of multidiscipline namely geological, geophysical, and petrophysical studies at different scale. The integrated studies will ultimately provide a comprehensive subsurface understanding and assisted in reservoir management decisions, data quality control, volumetric calculations, numerical simulation input, recovery factor forecast, and communication between disciplines are improved.

Database and Methodology

The methodology applied included core and thins section analysis, lithofacies description, paleoenvironment interpretation, HRSS interpretation, field scale stochastic static modeling, dynamic simulation and validation, and production forecasting. The lithofacies description was performed on 600 feet of core from 17 wells (Figure 1 and Figure 2) providing excellent areal and vertical datasets covering the studied area. More than 350 of thin sections were described to assess faunal contents and rock textures. Further integration with routine core analysis and mercury injection capillary pressure giving fundamental understanding on the composition, micro texture, pore system, lithofacies, and

diagenetic overprint of the reservoir. HRSS interpretation identified six fifth order parasequences that displayed aggradational, progradational, and retrogradational stacking cycles. In addition, conventional logs from more than 50 wells were employed.

Geological Setting and Reservoir Description

The studied oil field is situated onshore Abu Dhabi, it is a low relief four-way anticline closure cut by two strike slip fault systems namely N75W and N45W systems. The reservoir is part of Lekhwair Formation, which is part of the early transgressive sequence set of a second order supersequence. The reservoir belongs to the third order highstand sequence set. The fourth order parasequence sets show predominantly aggradational and progradational stacking patterns (Sharland, 2001; Strohmenger, 2006).

The studied field is in the northeastern part of the Arabian Plate which was covered by a giant shallow water carbonate platform essentially from the Permian to the Cretaceous (Sharland et al., 2001). The reservoir discussed in this paper is part of Lekhwair Formation, Thamama Group which was deposited in the intrashelf basin during Lower Cretaceous time (Valanginian). The basin was primarily formed because of environmental/climatic disturbances associated with global oceanic anoxic events.

During these times high subsidence rates caused the inability of carbonate sedimentation to keep up hence providing a shift from flat platforms to an emerging basin topography. Finally, it is postulated that the formation of another intra-shelf basin associated with the Valanginian Oceanic Anoxic Event was prevented by a regional tectonic uplift and platform exposure during the Late Valanginian (Vahrenkamp et al., 2015). These relatively shallow-water intra-shelf basins provided relatively high energy environments which were ideal settings for the creation of high-quality reservoir rock (Burchette, 1993).

The depositional geometry and lithofacies distribution comprise a well-exposed example of a transition from lagoon to ramp platform margin complex. Core, thin section, and well-log data were used to establish lithofacies distribution schemes and HRSS frameworks. Nine lithofacies were identified based on faunal content, texture, sedimentary structures, and lithologic composition. HRSS interpretation indicated six fourth order parasequences that displayed aggradational, progradational, and retrogradational stacking cycles (Figure 3).

The grain rich ooid-peloid shoal deposits exhibit the best permeability and oil saturation and it consists of discontinuous lithofacies body that depicts locally excellent porosity and permeability characteristics. The depositional geometry and lithofacies distribution comprise a well-exposed example of a transition from lagoon to ramp platform margin complex (Table 1 and Figure 4).

Regional multiphase tectonics processes are believed to be one of the main contributions for complex diagenetic trends in the studied field that in turn have resulted in variation in capillary pressure and reservoir rock types. The reservoirs generally have good reservoir characteristics at the crestal area and then gradually deteriorate at the flank area. The porosity and permeability degradation towards flank is thought to be strongly affected by late diagenetic process. Thin (2 to 5 feet) high permeability streaks are also presence with permeability value of more than 100 millidarcies (Figure 3).

Integrated Static Model Building Approach

The incorporation of recent seismic interpretations (horizons and faults), SCAL, core, log & well test data, production performance, and other available information is always done at the static modeling stage to reduce the reservoir uncertainties and improve the reliability of the reservoir model. Figure 5 shows innovative static modeling workflow that integrates stratigraphy, structural trend, and sedimentological/diagenetic process. It has been proven that this integrated methodology captured well the reservoir heterogeneity and provided a more robust dynamic model.

The important information carried by lithofacies models has a profound influence on reservoir heterogeneity. Geostatistics and stochastic simulation are tools to generate the multiple reservoir models that are defined by geologic, seismic, and production data. Caers and Zhang (2004) listed three goals of geostatistical reservoir characterization: (1) Provide reservoir models that depict a certain believed or interpreted geological heterogeneity; (2) Provide a quantification of uncertainty through multiple reservoir models, all honoring that same geological heterogeneity; (3) Integrate various types of data, each type.

The general workflow for the modeling of lithofacies and property distributions in sedimentary bodies involves three consecutive steps namely (1) reservoir geometry, (2) lithofacies, and (3) petrophysical properties constrained by lithofacies. These models are conditional to all available data and analog information (Deutsch, 2002). Geostatistical methods can reproduce various levels of geometric complexity while allowing for conditioning to a variety of site-specific data. TGS algorithm may be applied to construct stochastic facies models that reproduce spatial structures as shown by the variogram. The reservoir modeling workflow discussed in this paper including:

1) Input Data

The input data can be classified into two main types namely (1) hard data refer to lithofacies observed from core and thin section and (2) soft data serve as auxiliary conditioning data that correspond to statistical and geological parameters constraining lithofacies continuity such as: lithofacies proportions, variograms, training images, and conceptual depositional models. Soft data refers also to indirect measurements such as neural network result that is calibrated to lithofacies description.

2) The Construction of a Surface Based Framework

The first and largest scale of modeling is the construction of HRSS surfaces which were input to the model as gridded elevation surfaces. The objective is to establish large-scale of formation tops which create distinct zones. The zones built in the model correspond to the HRSS zonation described earlier. Using sequence stratigraphic concept, chronostratigraphic timelines, or boundaries (sequence boundary, flooding surface) were identified on core and became a basis for system tract identification. The identified chronostratigraphic boundaries on core are then tied to uncored wells by looking at distinctive well log character such as GR log. The reservoir zonation is in fact representing system tracts identified in the studied reservoir intervals (Figure 3). The main objective of this step is to identify and separate genetic units and tracts that were divided by a chronostratigraphic timeline.

3) Lithofacies Prediction by Neural Network on the Uncored Wells

Artificial intelligence and neural network methods have been applied to predicting lithofacies from logs on the uncored wells. The lithofacies described from cored wells were used as training data to see the relationship between relevant logs (GR, NPHI, RHOB) and lithofacies. The supervised lithofacies log on the wells was then QC'ed and compared to the original lithofacies. The result shows that high degree of similarity between original lithofacies and the resulted lithofacies log using neural network shows the reliability of the training data (Figure 6).

A single-layer neural network model was trained from digital well logs based on the available 10 described cored wells with the selected neural network parameters. This training data is then utilized to predict lithofacies on the supervised target wells. The neural network was trained using 100 maximum iteration, 5% error limit, 50% cross validation. The neural network models predict the lithofacies effectively. However, minor prediction errors in lithofacies curves, which are not observed in the core, were corrected according to core description, geological knowledge considering the general trend of lithofacies spatial distribution. The lithofacies curves are input to generate 3-D geostatistical models.

4) Lithofacies Data Analysis

Lithofacies Frequency Data. Although the propensity analysis based on the depositional setting can be very useful for reservoir delineation, it cannot give an accurate estimate of lithofacies probability in vertical sense. Hence lithofacies data from the cores and well logs can give not only lithofacies global frequency but also local frequencies. Figure 7 illustrates the lithofacies local frequency analysis of the studied reservoir. Each of the wells gives lithofacies relative frequencies at its location.

Lithofacies Lateral Trend Analysis. The lithofacies lateral trend analysis was based on the depositional characteristics and regional geology understanding. Such an analysis can include lithofacies depositional mechanism, spatial patterns, and object dimensions (Tucker and Wright, 1990). Based on the depositional conceptual model and petrophysical characteristics of the lithofacies, high quality reservoir rocks were obviously more likely found in the OPSG, SPPG, and BOB lithofacies of the shoal barrier. A conceptual lateral lithofacies distribution was shown earlier in Figure 4.

Lateral Variography Analysis. Variogram-based geostatistics is a traditional statistical method that uses variogram models and describes variations between different investigations or the spatial structure at any two spatial locations. These variogram models always try to capture information from two points of the available data; thus, variogram-based geostatistics modeling is also called two-point geostatistics (Deutsch and Journel, 1998) and it is a measure of lithofacies object dimensions (Jones and Ma, 2001). In the studied reservoir, the lithofacies patterns are complex and significant lateral heterogeneities are present. For example, shoal lithofacies (OPSG and SPPG) represents a relatively small and discontinue geometry. In contrast, the lagoon and ramp deposits are more continuous because they were deposited in relatively large scales. The lagoon deposits and ramp deposits have lateral major variogram from 4.5 kilometers to 16 kilometers (Figure 8). Care was taken to capture the dimension and morphology of carbonate bodies during variogram analysis and stochastically simulated geologic heterogeneity.

Vertical Lithofacies Proportions. Another important step in the lithofacies modeling is the elaboration of lithofacies maps in relation with the sequence stratigraphy framework. The vertical successions of lithofacies simply reflect depositional changes in a sequence. The stratigraphic reference class based on the hierarchy of sequences is a critical concept that links the description of a depositional lithofacies model and quantitative lithofacies frequency analysis. A first way to build a lithofacies map is to consider the most dominant lithofacies per sequence, resulting in distinctive retrograding and prograding trends, within which different lithofacies have been deposited. At a given a HRSS set, the relative frequency of each lithofacies can be calculated using all the wells or a group or cluster of wells. By stacking the lithofacies frequencies of all the depositional sequences, a vertical profile of the lithofacies relative frequencies is derived. Each relative frequency curve in such a profile represents one lithofacies proportion as a function of layers (or depth) and is termed the lithofacies vertical proportional curve (VPC). Such a vertical profile of lithofacies proportions represents an average stacking pattern for the wells used in the VPC calculations.

Global Vertical Profile of Lithofacies. The lithofacies VPC in Figure 9, generated using all the wells across the model area and stratigraphic sequences, represents global VPCs. Notice the difference in lithofacies presence in each sequence. The sequence 6 is dominated by lagoonal BSPP and AFEP lithofacies. Shoal barrier OPSG lithofacies reaches its peak in sequence 3. Lagoonal FPWP lithofacies appears at the top of the reservoir (sequence 1). The OPFR lithofacies (ramp deposit) appear to be increase in its proportion towards the top of sequences 3 and sequence 5. This represents change of the paleo-water depth over geological time. Cyclicity of the lithofacies assemblages implies sea level fluctuation and variation on the depositional environment through geological time. The degree of concordance between input and output data was also used as a quality control factor which was done separately for each sequence.

Sector or Local Vertical Stacking Profile of Lithofacies. A vertical profile of lithofacies relative frequencies can be generated by areas, sectors, or any group or cluster of wells. A VPC represents the facies relative frequencies as a function of depth within the selected area and/or cluster of the wells. Figure 10 shows examples of VPC variations at different parts of the field namely proximal, center, and distal parts of the basin. The VPC for each of the parts is different suggesting vertical and lateral lithofacies heterogeneity over the geological history and time. The OPPF lithofacies, for example, appears to be more intense on the western part of the field, particularly during cycle 5. In addition, the BOB lithofacies does not develop very well on the western part of the field. Each step which corresponds to one level of the HRSS hierarchy follows a specific modeling methodology adapted to its sedimentary features. Each systems tract (prograding, aggrading, retrograding) connects with a group of contemporaneous depositional systems and lithofacies products. In other words, each track shows distinctive vertical stacking of lithofacies. The vertical lithofacies trend in model was guided using vertical lithofacies probability curves that were derived from the vertical lithofacies proportion (Figure 9). With regards to the lateral distribution, two trends were applied namely (1) prograding (shallowing / HST) and (2) retrograding (deepening / TST).

Probability Maps Integrating Lithofacies Propensity and Frequency Data. Lithofacies frequency data based on the core and well logs typically represent only a small amount of the total population of a whole 3-D lithofacies model. Although a simple trend map was based on the depositional analysis, the trend is used in its spatial disposition based on the geologic lithofacies generating conditions and sedimentary depositional setup. Such a trend map is combined with lithofacies relative frequencies to define the probability. Thus, local proportions of the lithofacies relative to all the other lithofacies at the wells are the input frequency data for generating a probability map. As a summary, facies relative frequency, indicator variogram, and probability maps provide complementary information for describing the spatial distributions of depositional facies. For a given stratigraphic sequence, facies frequency determines their relative presence. While the variogram range

describes an average dimension of the facies objects, probability maps convey the facies spatial locations and associations. The combination of both vertical and lateral probability distribution will in turn provides insight into possible 3D conceptual lithofacies distribution during episodes of geological system tracts (Figure 11).

5) The Construction of Lithofacies Geometry and Distribution

The characteristics of the stochastic methods: 1) facies estimated at each grid cell directly depends on the facies estimated at the other cells; 2) the histogram for the resulting modelled property (or lithofacies proportions) is controlled by soft data, and can reproduce that of the original hard data; 3) spatial continuity of the resultant facies model is also controlled by soft data, and can reproduce that of the original hard data; 4) the main control on the modeled facies distribution is exerted by soft data. Stochastic methods discussed in this paper can fit either within pixel-based or object-based groups. All the object-based methods are stochastic methods, whereas pixel-based methods include either deterministic or stochastic methods.

Hybrid combination of OB and TGS algorithms were used. TGS is one of discrete variable modeling algorithms to stochastically model three-dimensional lithofacies architecture that are known to have sequential relationship in nature. Typical example includes progradational-aggradational-retrogradational patterns identified in the studied reservoirs. On the other hand, OB algorithm is powerful to model a discontinuous lithofacies body with no lithofacies ordering such as build up morphology of ooids grainstone (OPSG), peloidal grainstone (SPPG), and oncoidal boundstone (BOB). Therefore, the combination of the algorithms was able to capture distinctive lithofacies vertical and lateral trends. The resulting multirealizations demonstrated consistency with the regional geology, conceptual scheme, outcrop analogs, and geostatistical trend. (Figure 12).

Build up and discontinuous lithofacies morphology of OPSG, SPPG, and BOB was modeled simultaneously together with continuous and sequential lithofacies. Final lithofacies model realization (Figure 13 and Figure 14) captured the subsurface lithofacies heterogeneity. The shoal deposits covering 5% of the study area and contains interconnected, 5 to 8 kilometers long, 2 to 4 kilometers wide, and 1 to 4 feet thick shoal bodies. Variogram analysis indicates that the lithofacies distribution has a major direction of approximately N105ºE. Final lithofacies and depositional model reconstruction from the studied field indicated that the paleo shoreline of the basin during Valanginian was trending almost North-South. This interpretation is consistent with the previous regional studies and references of the studied area (Figure 15).

Variogram analysis indicates that the lithofacies distribution has a major direction of approximately N105ºE. Final lithofacies and depositional model reconstruction from the studied field indicated that the paleo shoreline of the basin during Valanginian was trending almost North-South. This interpretation is consistent with the previous regional studies and references of the studied area (Figure 15).

Further depositional and lithofacies trend evaluation suggests that the prograding trend shifting towards East during sea level fall period. In contrast, the retrograding trend shifting towards West during sea level rise time. The grainy shoal lithofacies (OPSG/SPPG) appears to be more concentrated on the western part of the field. On the other hand, the floatstone-rudstone lithofacies (ramp deposits) appears to be more abundant on the eastern part of the fields. This lateral trend combined with the vertical lithofacies proportion provided an insight that the paleo-shoreline should be oriented North-South and it was located somewhere towards the west of the field. Consequently, the distal (basin) area

would be towards the east of the field. This observation is consistent with the previous regional studies and references of the studied area (Sharland, 2001; van Buchem, 2002).

Property Modeling Approach

The established lithofacies distribution within HRSS framework was then used to constrain field-wide properties and diagenetic trend and distribution in the reservoir. Within each lithofacies, Sequential Gaussian Simulation (SGS) algorithm was employed to generate porosity distribution and then simulate permeability distribution conditional to porosity and RRT distribution. Considering the geological and diagenetic synthesis discussed above, a novel property modeling workflow was constructed. Reservoir property and their spatial distribution are the result of depositional environment, sedimentology, lithofacies, and diagenetic processes. Therefore, the subsequent property modeling was constructed following the pre-defined lithofacies distribution.

1) Reservoir rock type (RRT) Modeling

RRT is a process by which geological lithofacies are characterized by their dynamic behavior as dictated by rock fabric and texture, diagenetic overprint, and rock-fluid interaction (Gomes, 2008). Reservoir rock typing from core and log data was performed by integrating the routine core analysis (RCA) and mercury injected capillary pressure (MICP) of special core analysis (SCAL). It utilized relationship and classification of Porosity - Permeability, Capillary Pressure (Pc) - Water Saturation (Sw) and Pore throat radius (PTR). Well testing data in the reservoir interval was also incorporated to validate the water saturation of the studied reservoir. Discrete data analysis on RRT allowed in determining its vertical proportion curve within a lithofacies within a given HRSS set.

Rock type is related to inherent diagenetic unit; hence rock type is directly modeled as a pre-cursor of petrophysical modeling. 3D RRT was modeled using SIS algorithm and was conditioned to the pre-exiting lithofacies model due to the reason described above. To properly populate RRT spatial distribution, four (4) trends were incorporated during RRT modeling namely:

1. **Proportion Matrix.** Cross plot of porosity-permeability color coded by lithofacies obviously noticed that there is no one to one correlation between lithofacies and RRT (Figure 16a). Rock properties have been altered over long geological time and consequently a lithofacies could have more than one RRT. Therefore, the next important step is to quantify the frequency of each RRT for a lithofacies.

2. **Paleo-depth Trend.** Paleo-depth trend was applied in such a way the relatively good RRTs tend to appear on the crestal area while the relatively poor RRTs tend to be populated on the flank area. This is quite consistent with general property trend throughout the area (Figure 16b).

3. **Vertical RRT Trend.** The vertical trend in model was guided by vertical probability curves that were derived from the vertical RRT proportion (Figure 16c). This approach was utilized to ensure the vertical trend from well is captured in the model.

4. **High Permeability Streak Trend.** The high permeability streak is equivalent to RRT 7. Detail thin section and core observations reveal that the high permeability streaks with values of >100 mD (Figure 16d) occur only on a shoal lithofacies (OPSG/SPPG) that is in the oil pool. Shoal that is in the aquiver experiencing cementation hence its permeability is deteriorated.

2) Porosity Modeling

Rock Type is related to inherent diagenetic unit; hence Rock Type was directly modeled as a pre-cursor of petrophysical modeling. Porosity modeling was built using effective porosity (PHIE) logs. Porosity conditional to well log and hierarchical trend model as a local variable mean of the model. Algorithm used for porosity distribution was Sequential Gaussian Simulation (SGS) conditioned to the pre-existing RRT distribution (Figure 5). It is also conditioned to the reference target global distribution and the variogram, and independently for each RRT in the reservoir. In the porosity modeling workflow, paleo-depth trend was applied as well. This aligned with general property trend throughout the studied area. As such, porosity distribution will honor both RRT distribution as well as deterioration trend towards flank area.

SGS assigns a value to each grid cell sequentially, by following a preset path visiting all the modelling grid nodes (Deutsch and Journel, 1998). The assignation is made by random sampling from a PDF function, which is calculated for each grid node by assuming a Gaussian distribution described by the mean value and the standard deviation predicted by kriging interpolation and variograms. SGS requires the modeling of semivariograms of the Gaussian transform of the data. The experimental semivariograms were calculated for each RRT. The semivariograms were modeled by a spherical and a Gaussian nested structure (Figure 17).

3) Permeability Modeling

To proceed into the permeability model, RRT also becomes important. Different RRT will have different porosity-permeability distribution. Hence to model permeability, initial emphasis was placed on its derivation from porosity using deterministic Porosity-Permeability transforms established per RRT classes. Algorithm used for permeability population was SGS conditioned to the pre-existing RRT model. In this method, the permeability distribution was simulated with porosity realization as secondary property for collocated cokriging and it was populated using porosity-permeability bivariate cloud transform which is unique for each rock type. By doing this, the permeability range will reproduce cloud variation as shown by logs and routine core analysis well data. This methodology honors the available well-log porosity, permeability from log and core, the trend in the porosity and permeability given by geologic information on the transition in lithofacies, and the geometry of RRT. The histogram or probability distribution of permeability is honored within each RRT by the constraint to honor the bivariate distribution of permeability with porosity.

The final permeability distribution is one of key factors that controlling the fluid flow behavior. Performance of reservoirs is strongly dependent on the spatial distribution of permeability. A homogeneous permeability distribution would have significantly different flow characteristics compared to a model showing spatial correlation.

In geostatistics, the variogram (Figure 17) is commonly used a measurement of spatial correlation inferred from the available data such as core, geological understanding, and spatial correlation. In general, by constraining the permeability model to the porosity-permeability plot and the

reference variogram for each RRT then the spatial distribution of permeability is adequately controlled. The robustness of the porosity-permeability transforms has been blind tested in some cored wells by generating permeability profiles from these transforms and by comparing the calculated values back with the corresponding core measured permeability profiles.

Complete modeling realization integrating sequence stratigraphy, paleostructural trend, and sedimentological/diagenetic process is shown in Figure 18a, 18 b, 18c. Overall, the property model result reflected the complex geological setting very well.

4) Saturation Modeling

Saturation height model with utilization of core and logs data was used to provide an accurate water saturation distribution at well scale as well as at reservoir model scale (Figure 18d). To solve this issue then saturation height functions (Skelt-Harrison) were created for each of the RRTs. Open hole saturation log and production data were used to validate the functions.

Flow Simulation and History Match Validation

The studied reservoir discussed in this paper is unsaturated reservoir with not significant variation of fluid properties both areal and vertically. Existing producer wells are 80% horizontal and the remaining 20% are vertical to deviated producers. The production history is the approximately 20 years and currently a peripheral water injection is implemented, all injector wells are horizontals. The objective of the dynamic model was to create a reservoir simulation to reproduce the historical production data and the pressure behavior of the reservoirs. Additionally, the reservoir simulation model is integrating the static model with a new saturation height function, EOS, and relative permeability information.

The EOS of the model was generated matching all existing conventional PVT data and three advance PVT studies, considering swelling tests and minimum miscibility pressure with CO_2 and miscible rich hydrocarbon. For the relative permeability, existing laboratory data was classified by rock type and analyzed. Correlations were created considering a relative permeability end points for each RRT and using modified Corey correlation, a complete set of simulation input was generated. For capillary pressure, the model was initialized considering capillary pressures from saturation high function results for each RRT. For the water saturation distribution (Figure 19), the saturation height function for each RRT was determined based on Skelt-Harrison.

Full Field history match is shown in Figure 20. One of the main improvements of this new reservoir model is its ability to reproduce the reservoir pressure in the center of the reservoir which is an indication of the limited connection between injectors and producers (Figure 21). After a good history match was achieved, prediction cases were run considering different field development plan options and implementation time. The cases considered for prediction are: No further action (NFA), gas lift implementation, infill drilling, conversion of water injection project from peripheral to pattern and EOR cases considered are CO_2 and rich hydrocarbon injection as continuous and WAG.

Results and Conclusion

- An integrated approach utilizing sequence stratigraphic technique, lithofacies and depositional interpretation, diagenetic analysis, and geostatistics provide robust insight for better understanding on the complex reservoir.
- The combination of TGS and OB algorithms was able to model complex lithofacies transition in the studied reservoir. The resulted base case geostatistical model was sent to the simulator and the resulting dynamic model portrayed a satisfactory match to the actual production data (Figure 2). Hence it will provide reliable production forecast and to optimize the current reservoir management plan ensuring optimal sweep efficiency and recovery.
- For petrophysical modeling, pixel-based SGS algorithm with a specific data transformation and trends can help to capture the variations of petrophysical properties in different lithofacies.
- Equiprobable multirealizations of the static model were created including lithofacies, rock types, porosity, permeability, and water saturation. The models were evaluated visually and statistically to select a single realization for use in the next simulation model. The resulted base case geostatistical model was sent to simulator and the resulting dynamic model portrayed a satisfactory match to the actual production data. Hence it will provide reliable production forecast and to optimize the current reservoir management plan ensuring optimal sweep efficiency and recovery.

Acknowledgements

The authors thank the management of ADNOC (Abu Dhabi National Oil Company) Onshore for authorizing the publication of the data in this paper.

Nomenclature

EOR	Enhance Oil Recovery
EOR	Equation of State
HRSS	High Resolution Sequence Stratigraphy
HST	Highstand Systems Tract
MICP	Mercury Injected Capillary Pressure
NMR	Nuclear Magnetic Resonance
NPHI	Neutron Porosity
OB	Object Based
PTR	Pore Throat Radius
RCA	Routine Core Analysis
RHOB	Bulk Density
RRT	Reservoir Rock Type
SB	Sequence Boundary
SCAL	Special Core Analysis

SGS	Sequential Gaussian Simulation
TGS	Truncated Gaussian Simulation
TST	Transgressive Sequence Tract
PDF	Probability Distribution Function

References Cited

Bosence D.W.J., 2005. A new, genetic classification of carbonate platforms based on their basinal and tectonic setting in the Cenozoic. Sediment Geology 175:49–72.

Bosence D.W.J., et al. 1998. Architecture and depositional sequences of Tertiary fault-block carbonate platforms; an analysis from outcrop and computer modeling. Marine Petroleum Geology 15:203–211.1.

Burchette, T. P. 1993. Mishrif Formation (Cenomanian–Turonian), Southern Arabian Gulf: carbonate platform growth along a cratonic basin margin, in J. A. T. Simo, R. W. Scott, and J. P. Masse, eds., Cretaceous carbonate platforms. AAPG Memoir 56, p. 185–199.

Caers, J. and Zhang, T. 2004. Multiple-point geostatistics: A quantitative vehicle for integrating geologic analogs into multiple reservoir models, in Grammer, G.M., Harris, P.M.M., and Eberli, G.P., eds., Integration of outcrop and modern analogs in reservoir modeling. AAPG Memoir 80, p. 383-394.

Deutsch, C.V. 2002. Geostatistical Reservoir Modeling. Applied Geostatistics Series, New York, Oxford University Press, 376 pp.

Deutsch, C.V. and Journel, A. 1998, GSLIB: Geostatistical Software Library and User‘s Guide, 2nd ed.: New York, Oxford University Press, p. 369.

Dunham, R.J. 1962. Classification of Carbonate Rocks According to Depositional Texture. AAPG Memoir 1, p 108-121.

Gomes, J.S., et al. 2008. Carbonate Reservoir Rock Typing – The Link between Geology and SCAL. Presented at the SPE ADIPEC. SPE-118284.

Jones, T.A. and Ma, Y.Z. 2001. Geologic characteristics of hole-effect variograms calculated from lithology-indicator variables: Mathematical Geology, v. 33, no. 5, p. 615–629, doi: 10.1023/A: 1011048913041.

Journel, A.G. and Ying, Z. 2001. The theoretical links between Sequential Gaussian Simulation, Gaussian Truncated Simulation, and Probability Field Simulation. Mathematical Geology, 33, 31-39.

Leverett, M.C. 1941. Capillary Pressure Behaviour of Porous Solids. AIME, Vol 142, pp. 151-169.

Pittman, E.D. 1992. Relationship of Porosity and Permeability to Various Parameters Derived from Mercury Injection Capillary Pressure Curves for Sandstone. AAPG Bulletin, Vol 76, No 2, pp 191-198.

Rebelle, M. and Al Nuaimi, M.A. 2006. Lithofacies, Depositional Environment, and High-Resolution Sequence Stratigraphy interpretation of Reservoir 1, 2, 3, Field A. ADCO Internal Report.

Salahuddin, A.A., et al. 2015. Innovative Integration of Subsurface Data and History Matching Validation to Characterize and Model Complex Carbonate Reservoir with High Permeability Streaks and Low Resistivity Pay Issues, Onshore Abu Dhabi. Presented at the SPE RCSC. SPE-175682.

Scholle, P. A., and Ulmer-Scholle, D. S. 2003. A Color Guide to the Petrography of Carbonate Rocks: Grains, Textures, Porosity, Diagenesis, AAPG Memoir 77 (Vol. 77).

Scholle, P.A. 1978. A Color Illustrated Guide to Carbonate Rock Constituents, Textures, Cements, and Porosities. AAPG Memoir 27.

Sharland, P.R., et al. 2001. Arabic Plate Sequence Stratigraphy. GeoArabia Special Publication 2. Gulf PetroLink, Bahrain, 371 p.

Strohmenger, C.J., et al. 2006. High-Resolution Sequence Stratigraphy and Reservoir Characterization of Upper Thamama (Lower Cretaceous) Reservoirs of a Giant Abu Dhabi Oil Field, United Arab Emirates. AAPG Memoir 88 / SEPM Special Publication.

Strohmenger, C.J., et al. 2004. High-Resolution Sequence Stratigraphy of the Kharaib Formation (Lower Cretaceous, UAE). Presented at the SPE ADIPEC. SPE-88729.

Tucker, M.E. and Wright, V.P. 1990. Carbonate sedimentology: Oxford, Blackwell Scientific Publications, 482 p.

van Buchem F.S.P., et al. 2002. High-Resolution Sequence Stratigraphic Architecture of Barremian/Aptian Carbonate Systems in Northern Oman and the United Arab Emirates (Kharaib and Shu`aiba formations). GeoArabia, Vol 7, No 3, pp. 461-500.

Vahrenkamp, V.C., et al. 2015. Late Jurassic to Cretaceous Source Rock Prone Intra-Shelf Basins of the Eastern Arabian Plate – Interplay between Tectonism, Global Anoxic Events and Carbonate Platform Dynamics. Presented at the IPTC. IPTC-18470-MS.

Wagoner, J.C.V., et al. 1990. Siliciclastic Sequence Stratigraphy in Well Logs, Cores, and Outcrops: Concepts for High-Resolution Correlation of Time and Fades. AAPG Methods in Exploration Series No. 7.

Zhang, T. 2008. Incorporating geological conceptual models and interpretations into reservoir modeling using multiple-point geostatistics: Earth Science Frontiers, v.15, no.1, p. 26-35.

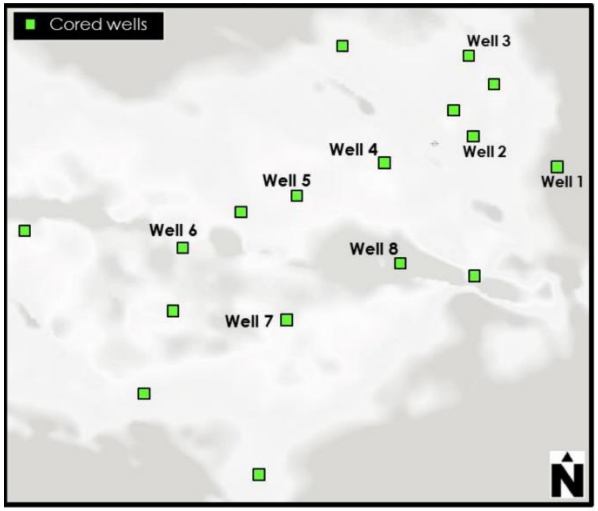

Figure 1. Reservoir-1 depth map and cored wells location. Some key cored wells are numbered.

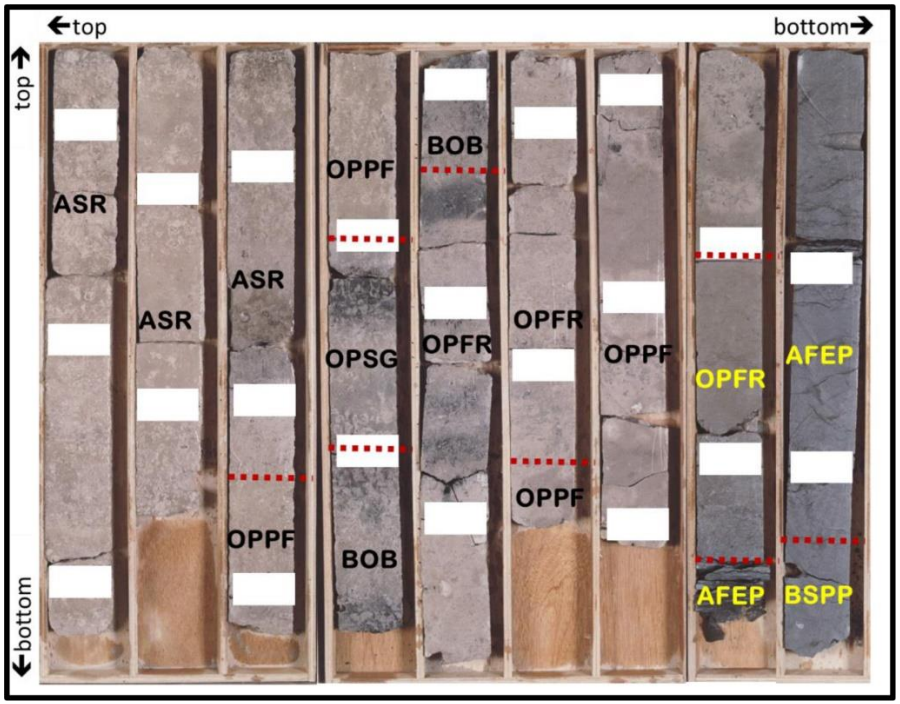

Figure 2. Core description from one of the cored wells showing vertical lithofacies succession.

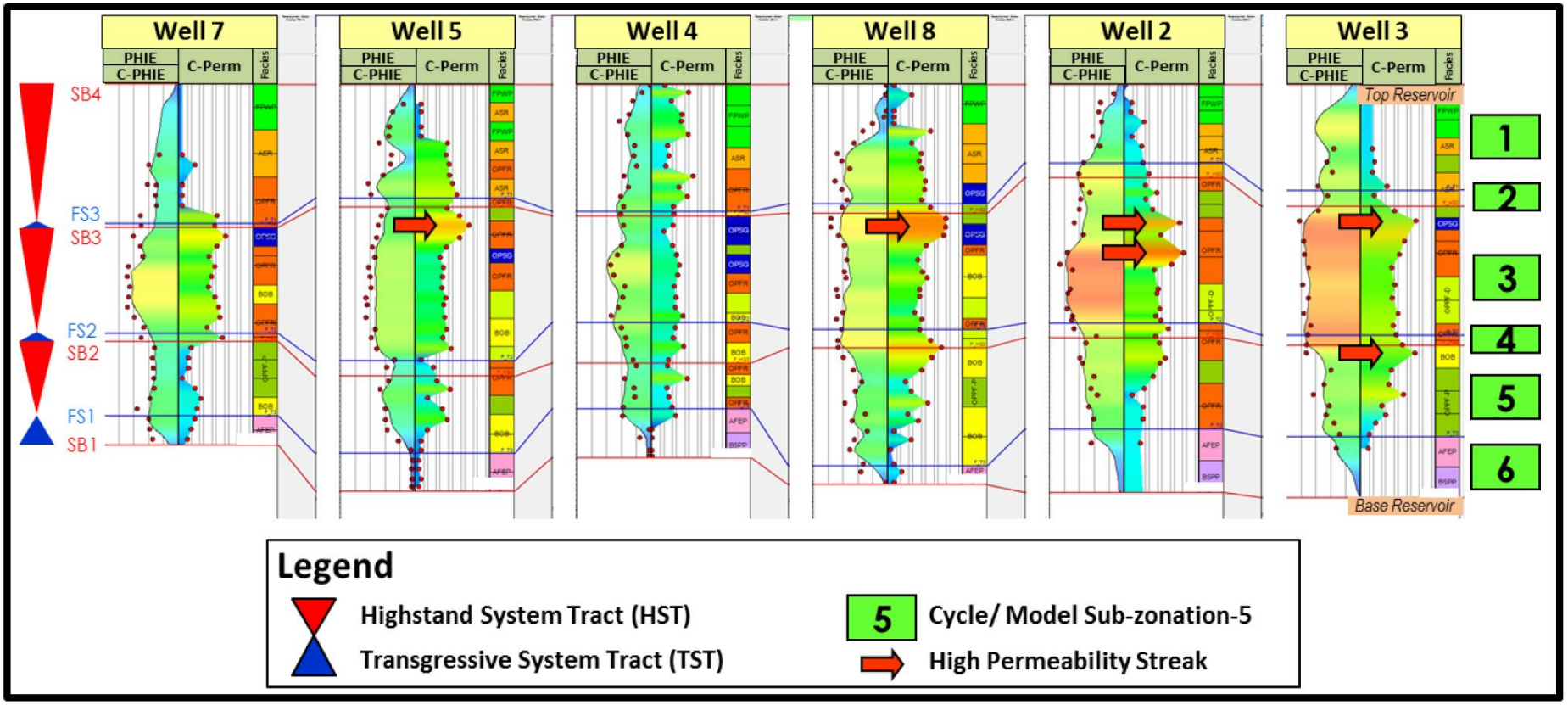

Figure 3. Cross section on some key cored wells showing the established HRSS framework and the vertical and horizontal distribution of lithofacies. Red arrow indicates high permeability streak with permeability value of more than 100mD.

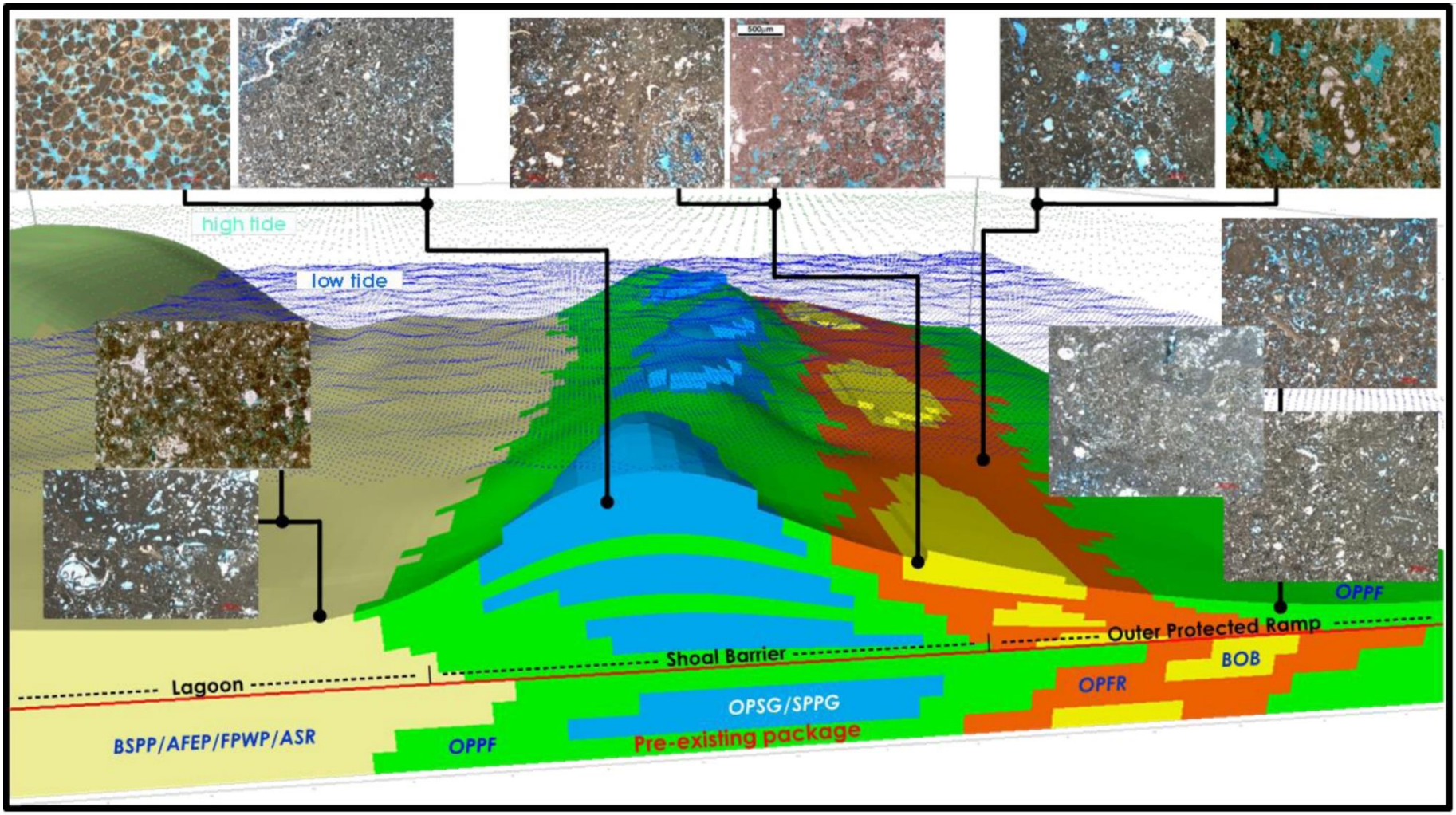

Figure 4. Paleobathymetric profile showing the interpreted depositional environment, lateral lithofacies distribution, and thin section photography of the studied reservoir.

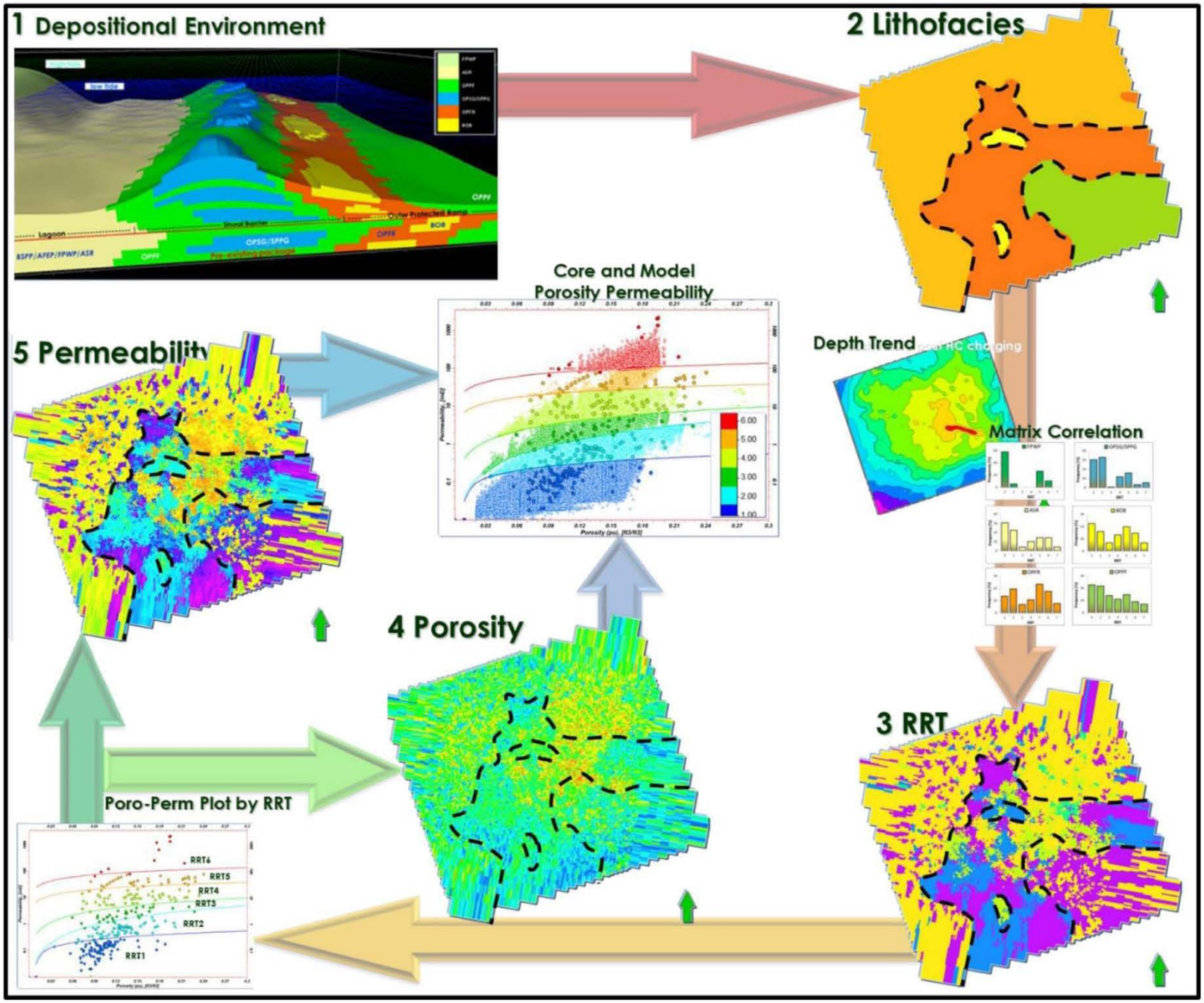

Figure 5. Static modeling workflow, integrating sequence stratigraphy, structural trend, and sedimentological / diagenetic processes.

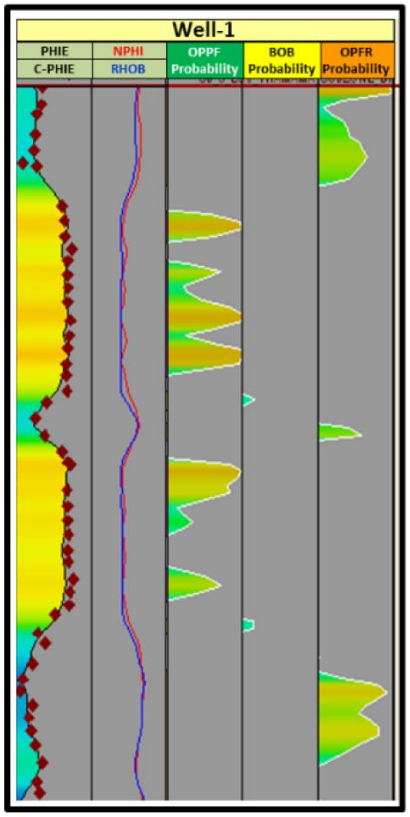

Figure 6. Facies prediction using supervised neural network.

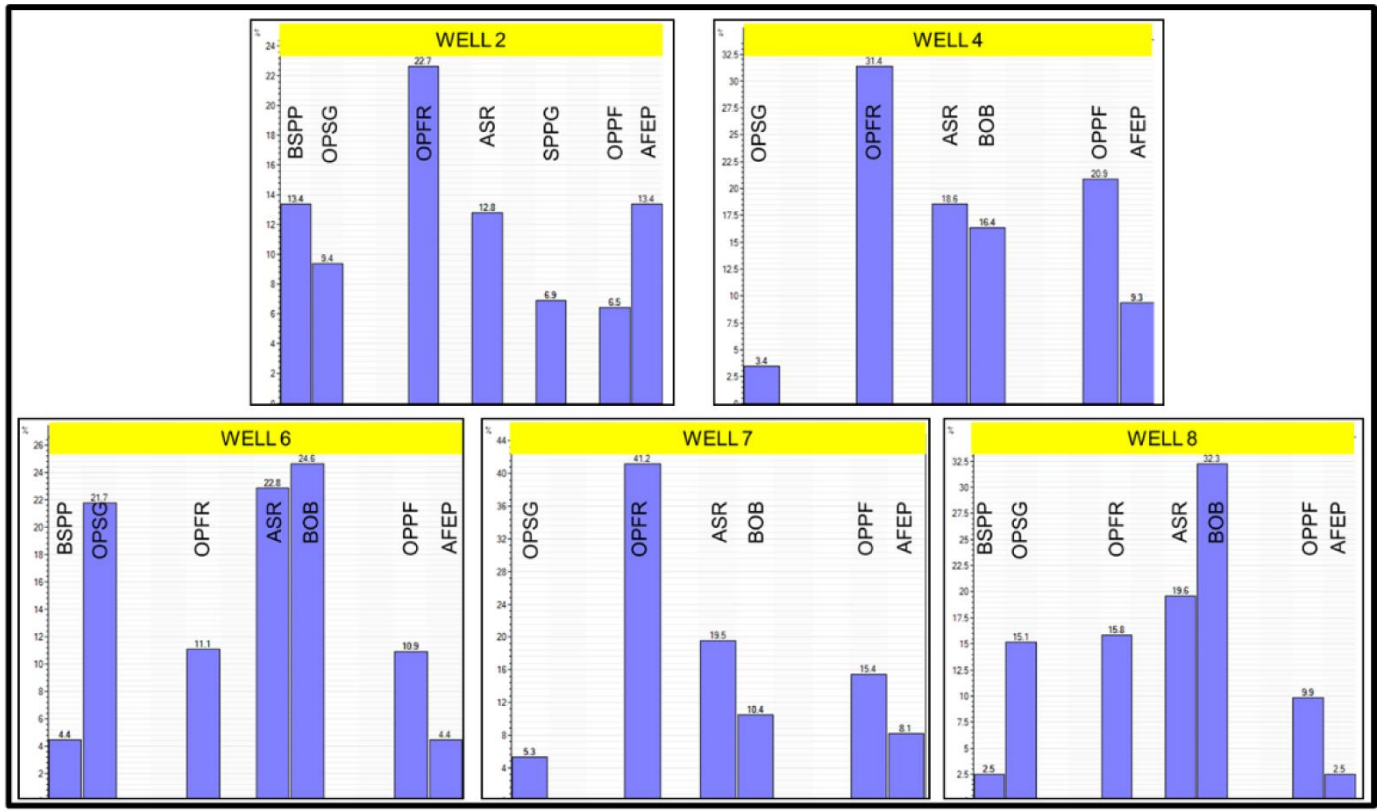

Figure 7. Histogram of lithofacies global frequencies from some cored wells.

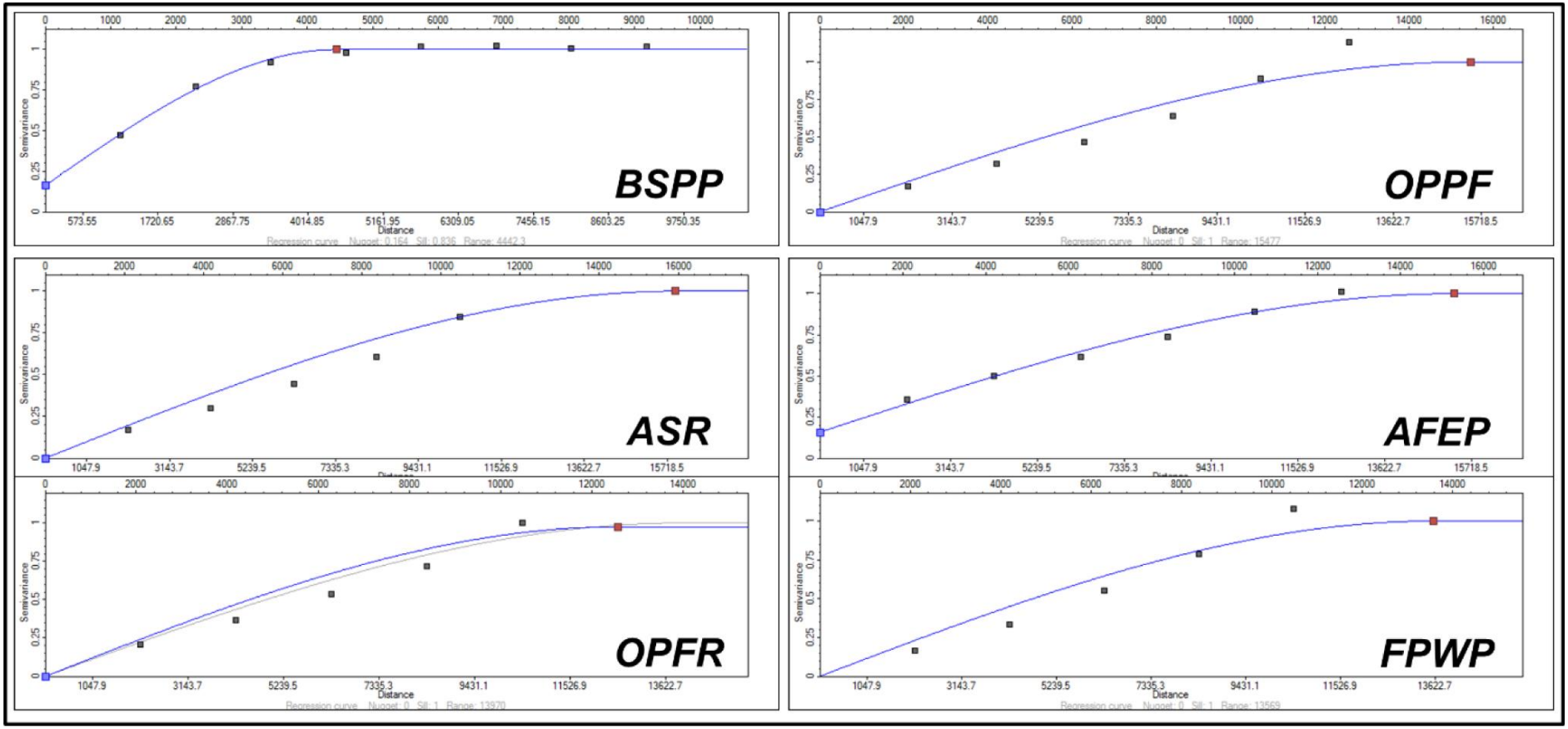

Figure 8. Lithofacies variograms in the NE-SW direction with a range of 4500 meters for BSPP lithofacies to 16,000 meters for ASR lithofacies. Nugget effect of 0 to 0.16. Lag distance is in meters.

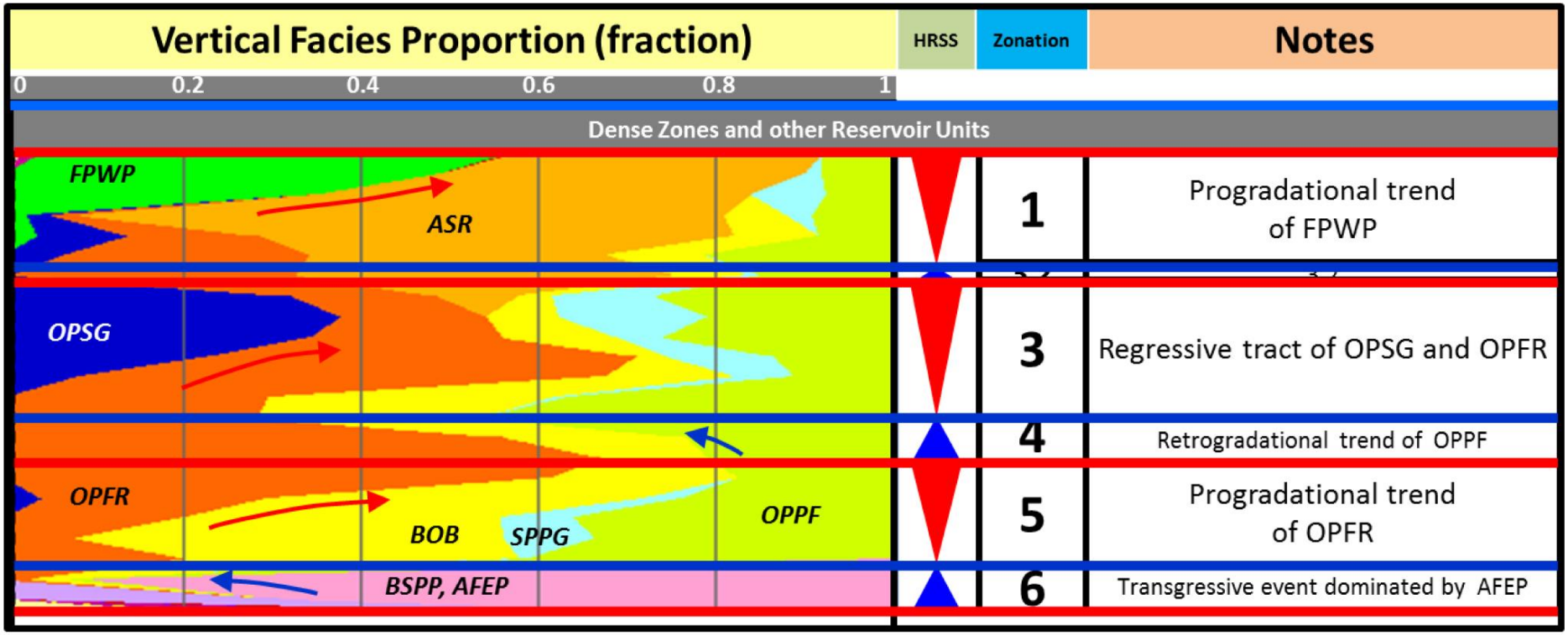

Figure 9. Global vertical stacking profiles of the lithofacies proportions versus depth (layer). It shows dominant lithofacies per sequence, resulting in distinctive retrograding and prograding trends.

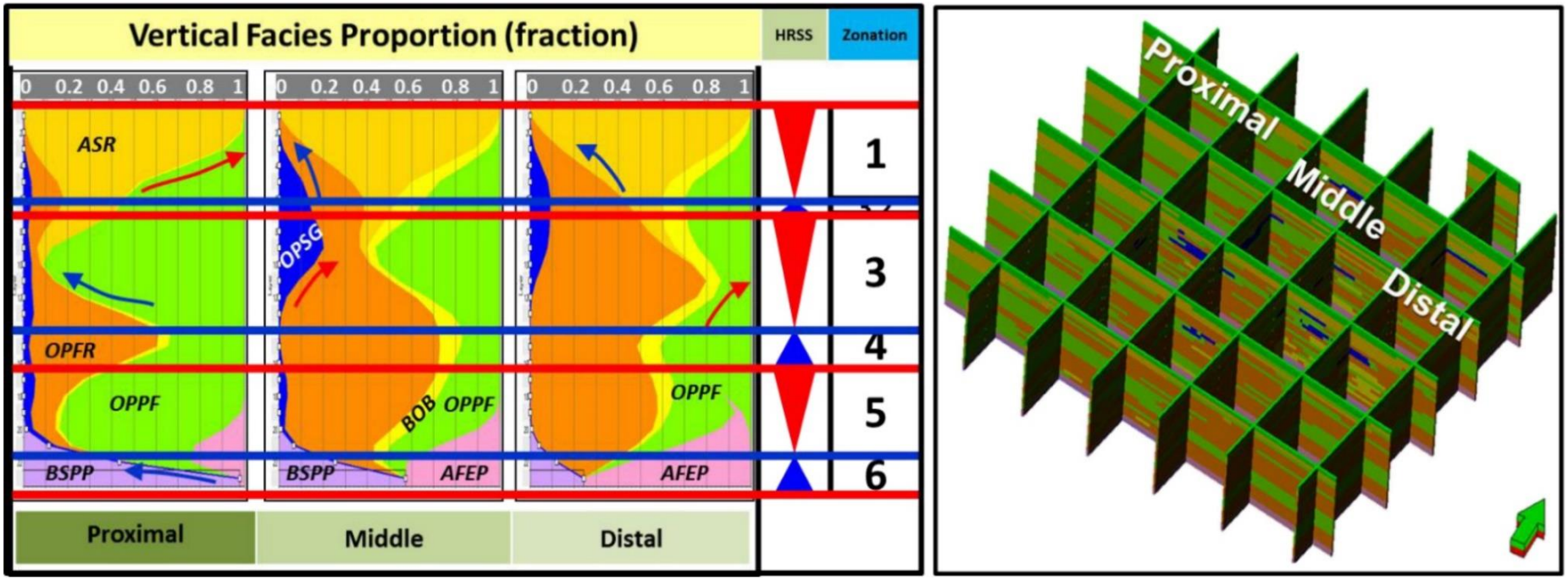

Figure 10. Vertical stacking profiles of the lithofacies proportions versus depth (layer) at different parts of the field namely proximal, middle, and distal part of the basin. Notes how all the lithofacies change vertically and laterally.

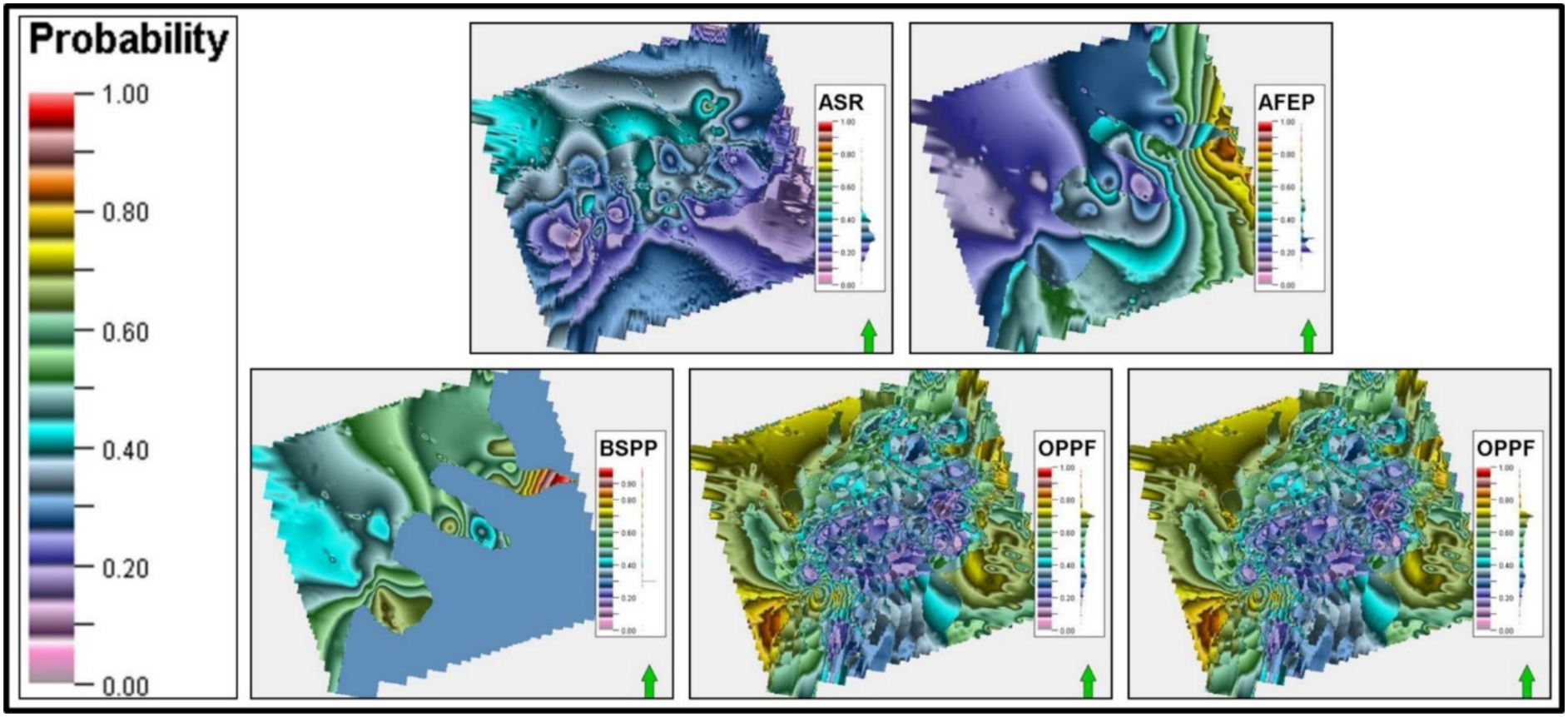

Figure 11. The lithofacies probabilities, example from lithofacies.

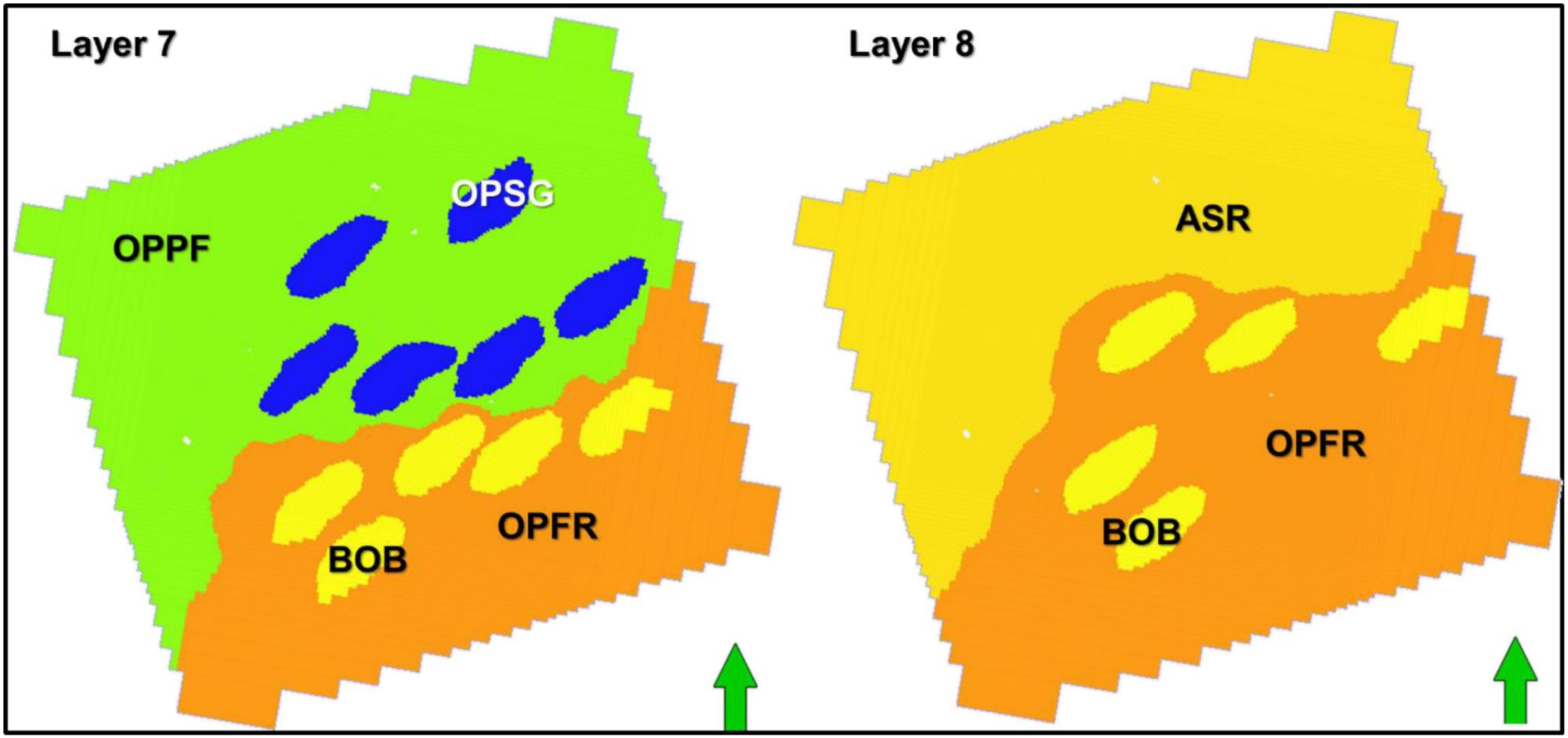

Figure 12. Object-based realization for OPSG and BOB lithofacies.

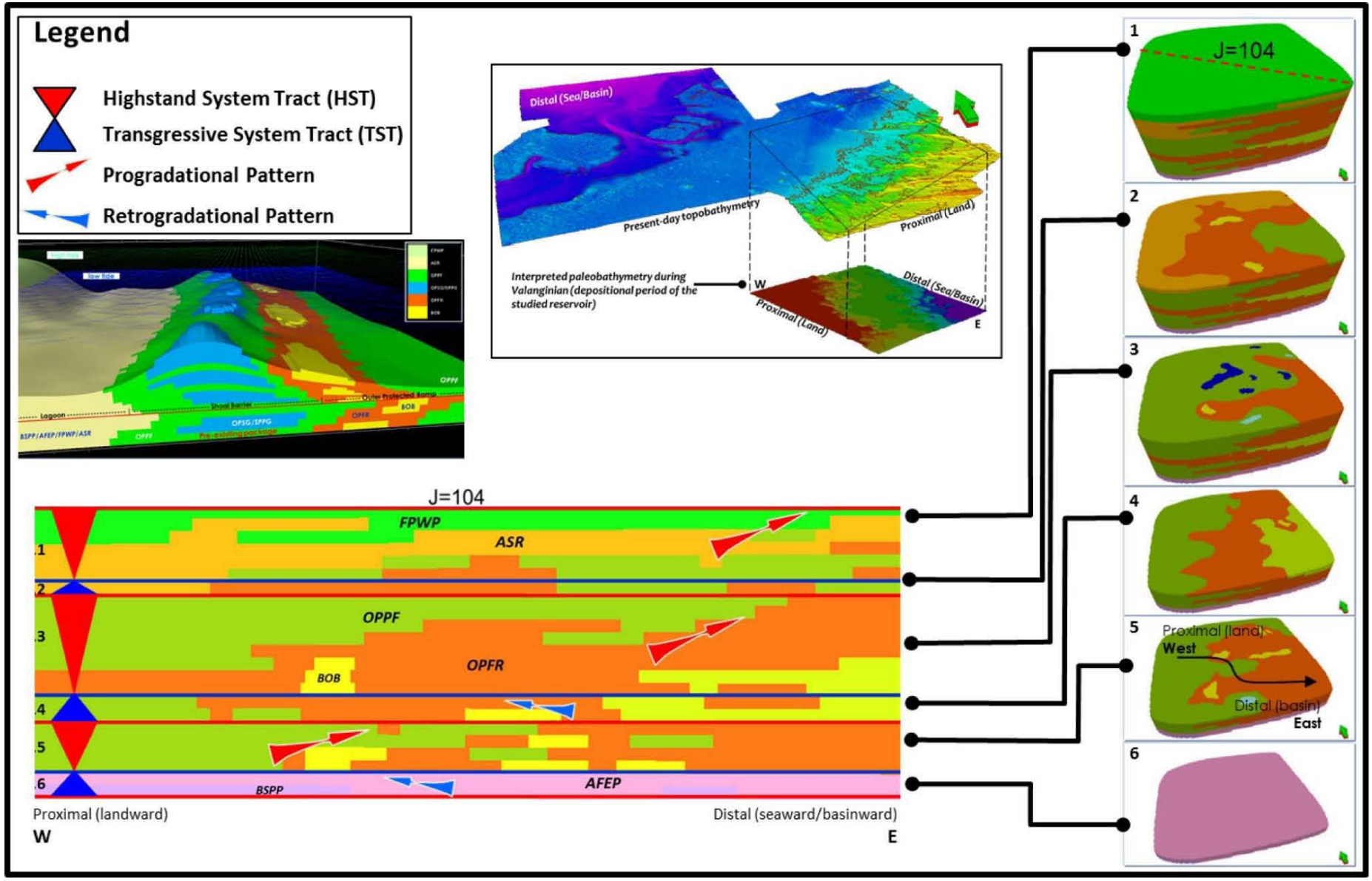

Figure 13. Lithofacies model distribution and its evolution through geological time. The 3D lithofacies model was generated by utilizing HRSS-based zonation to separate lithofacies genetic units and their distinctive system tracts.

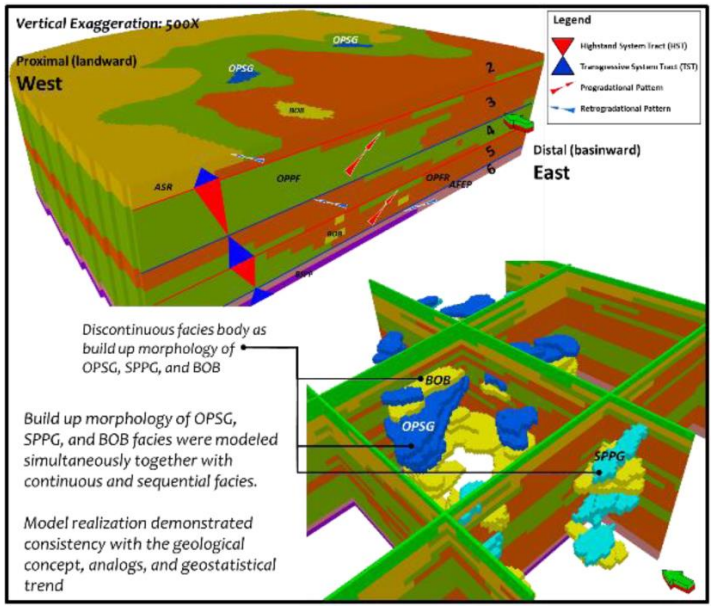

Figure 14. Complete three-dimensional lithofacies realization. Build up and discontinuous lithofacies morphology was modeled simultaneously with continuous and sequential lithofacies which is consistent with the concept, analogs, and geostatistical trend.

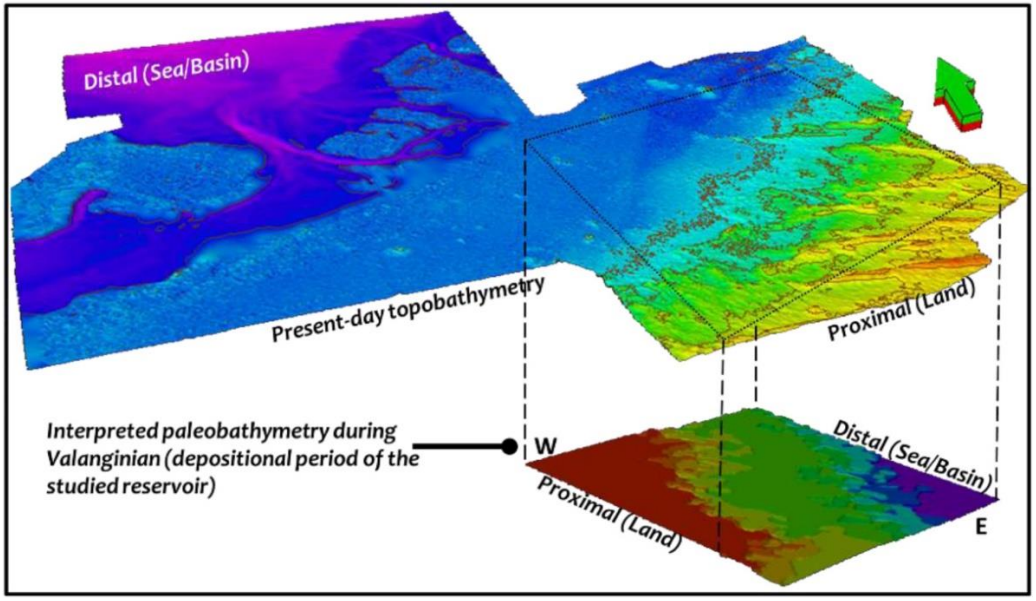

Figure 15. Interpreted North-South trending paleo-bathymetry during deposition of the three studied reservoirs (Valanginian time) as inferred from 3 dimensional lithofacies and depositional environment reconstruction. Contrarily, the present-day topobathymetry is trending almost East-West.

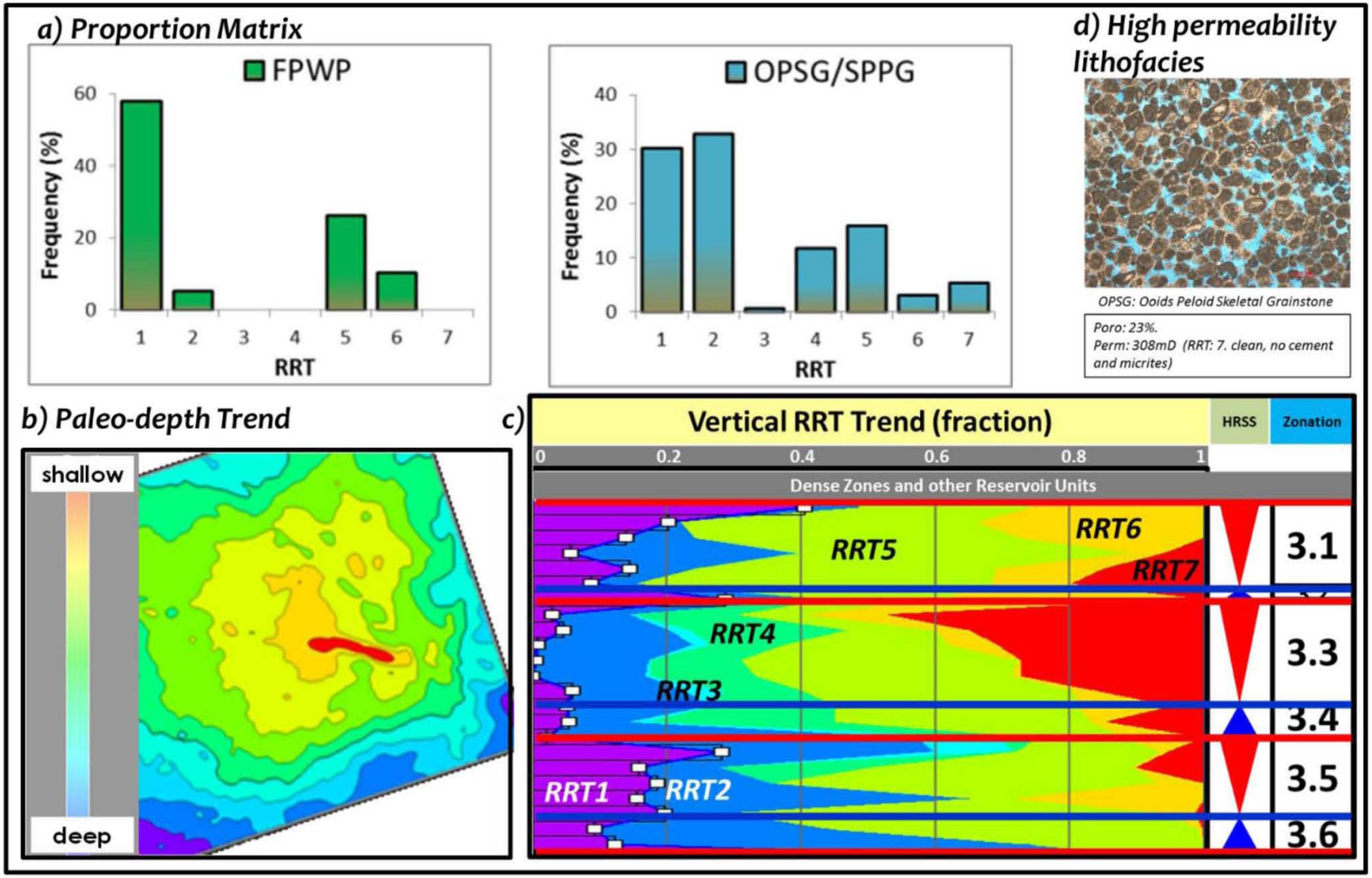

Figure 16. Trends that were incorporated for constraining RRT spatial distribution: a) Proportion Matrix; b) Paleo-depth Trend; c) Vertical RRT Trend; high permeability lithofacies.

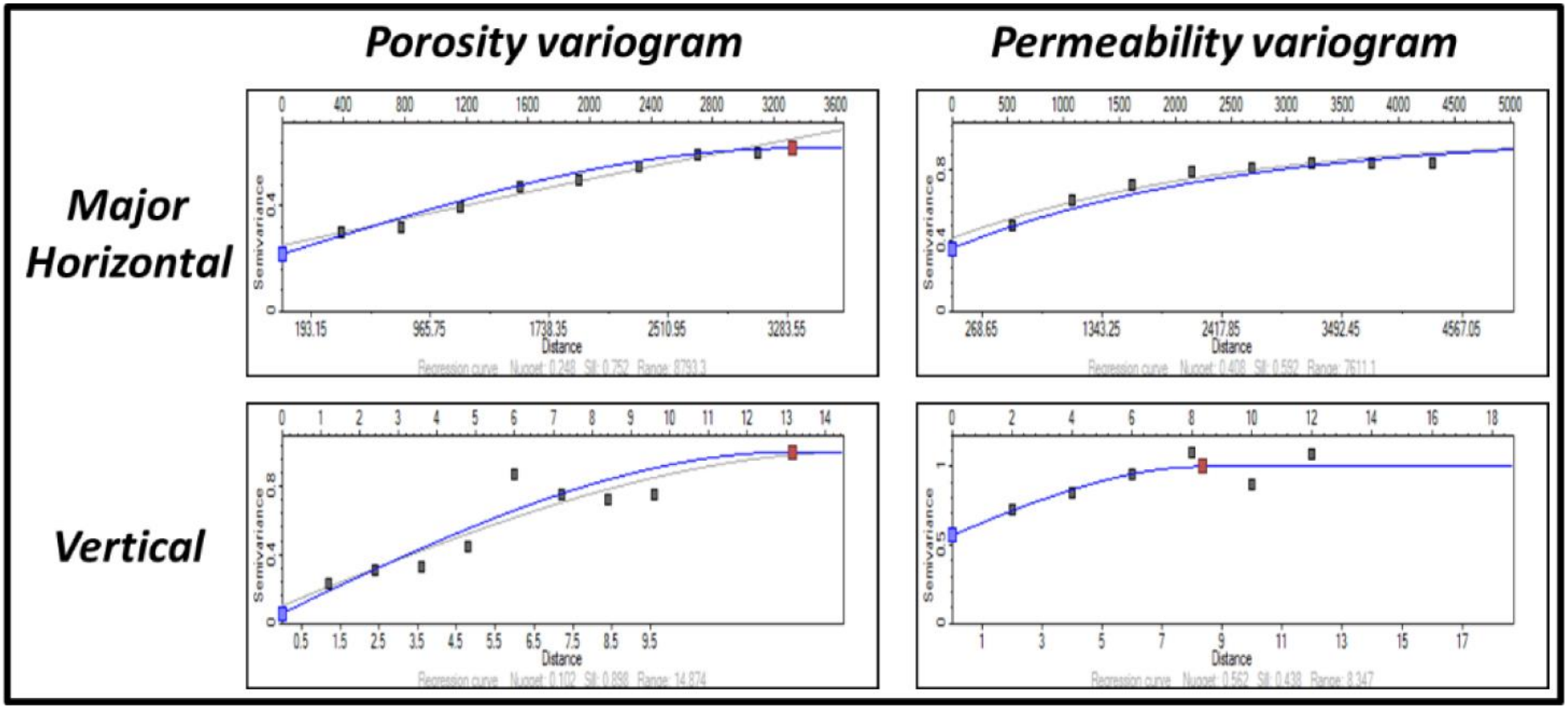

Figure 17. Horizontal and vertical variograms of the Gaussian transform of the porosity and permeability data.

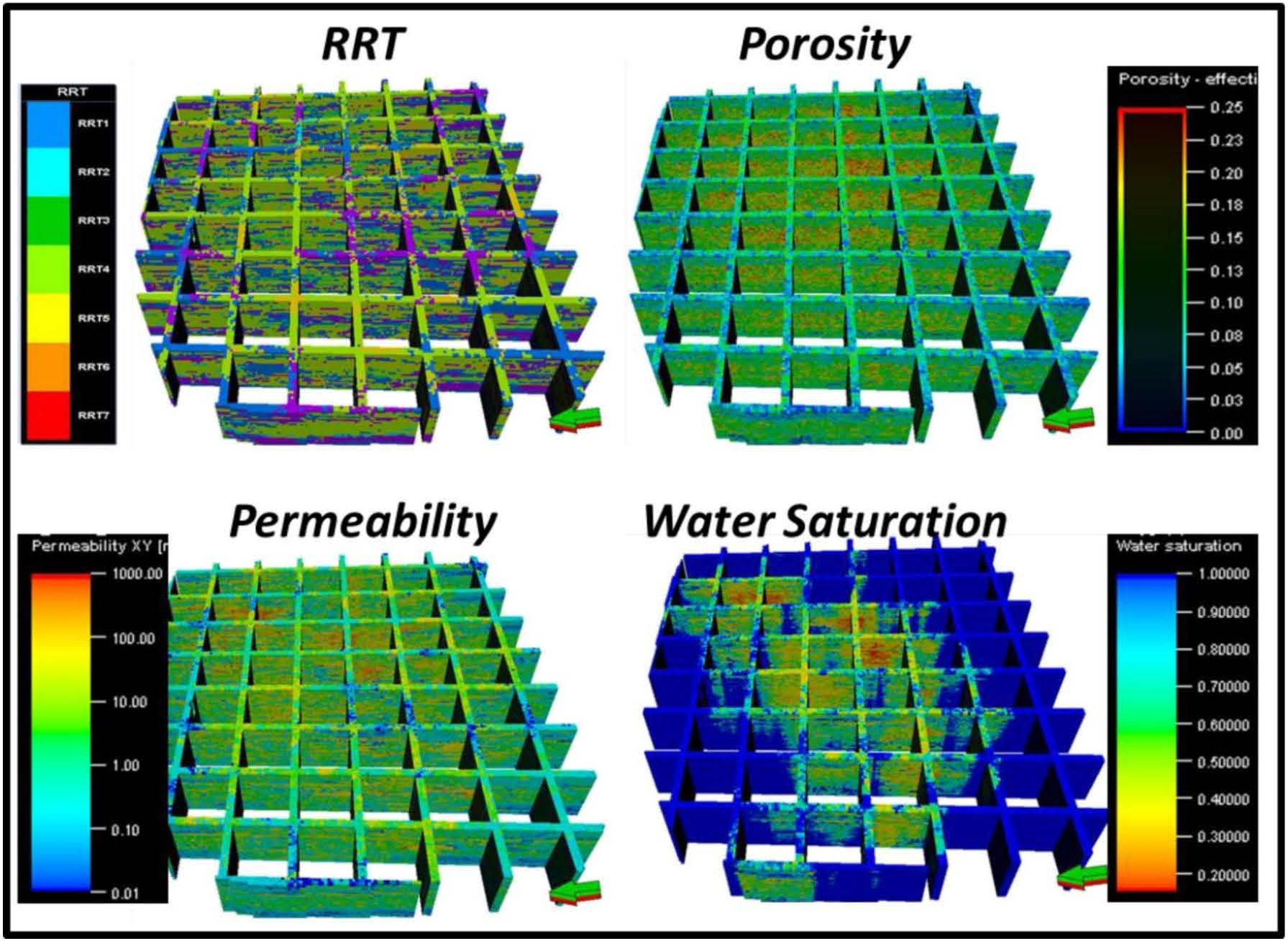

Figure 18. Fence diagrams of the RRT, porosity, permeability, and SW realizations (simbox view).

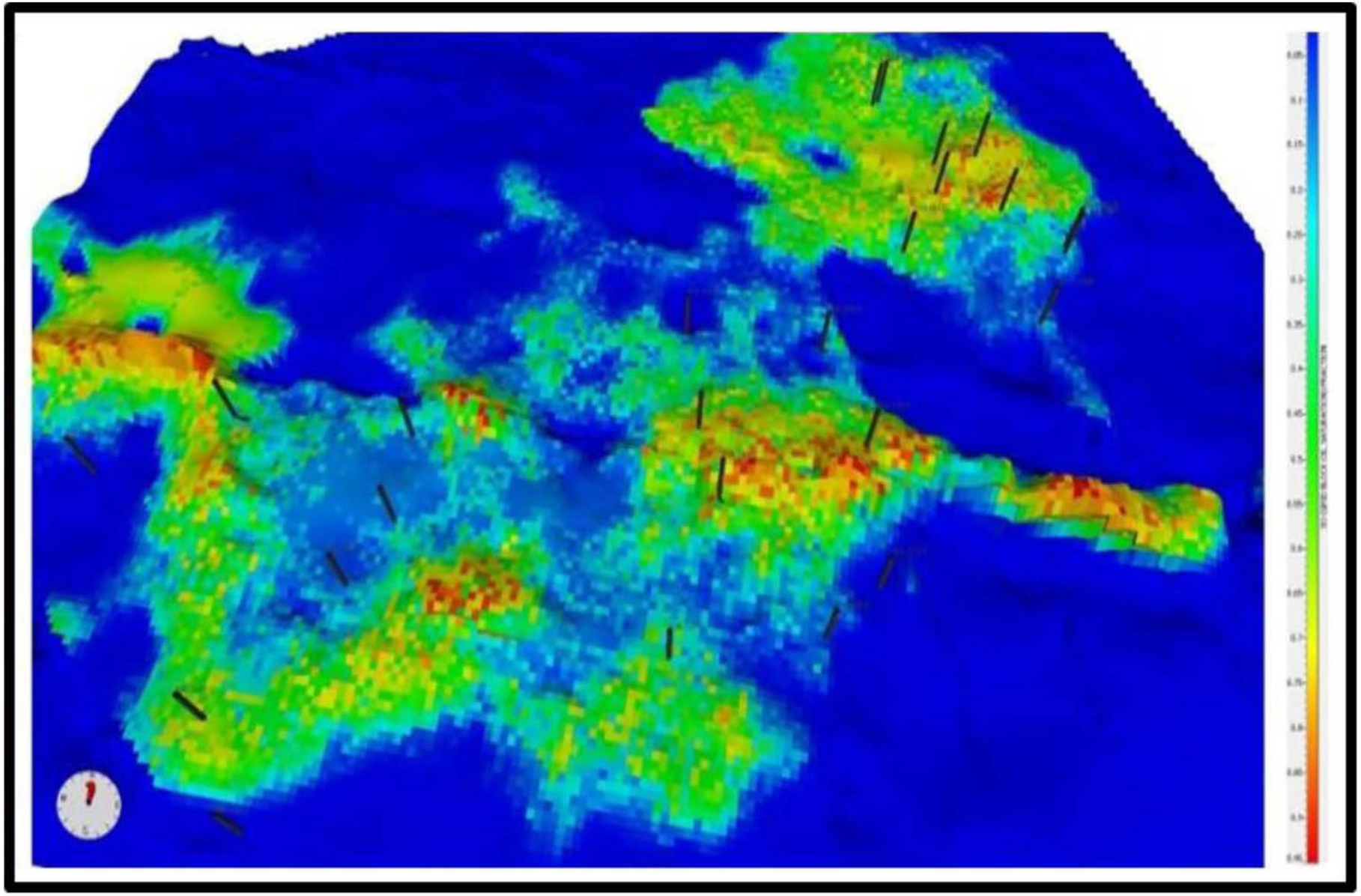

Figure 19. a plan view of the initial fluid distribution in the model.

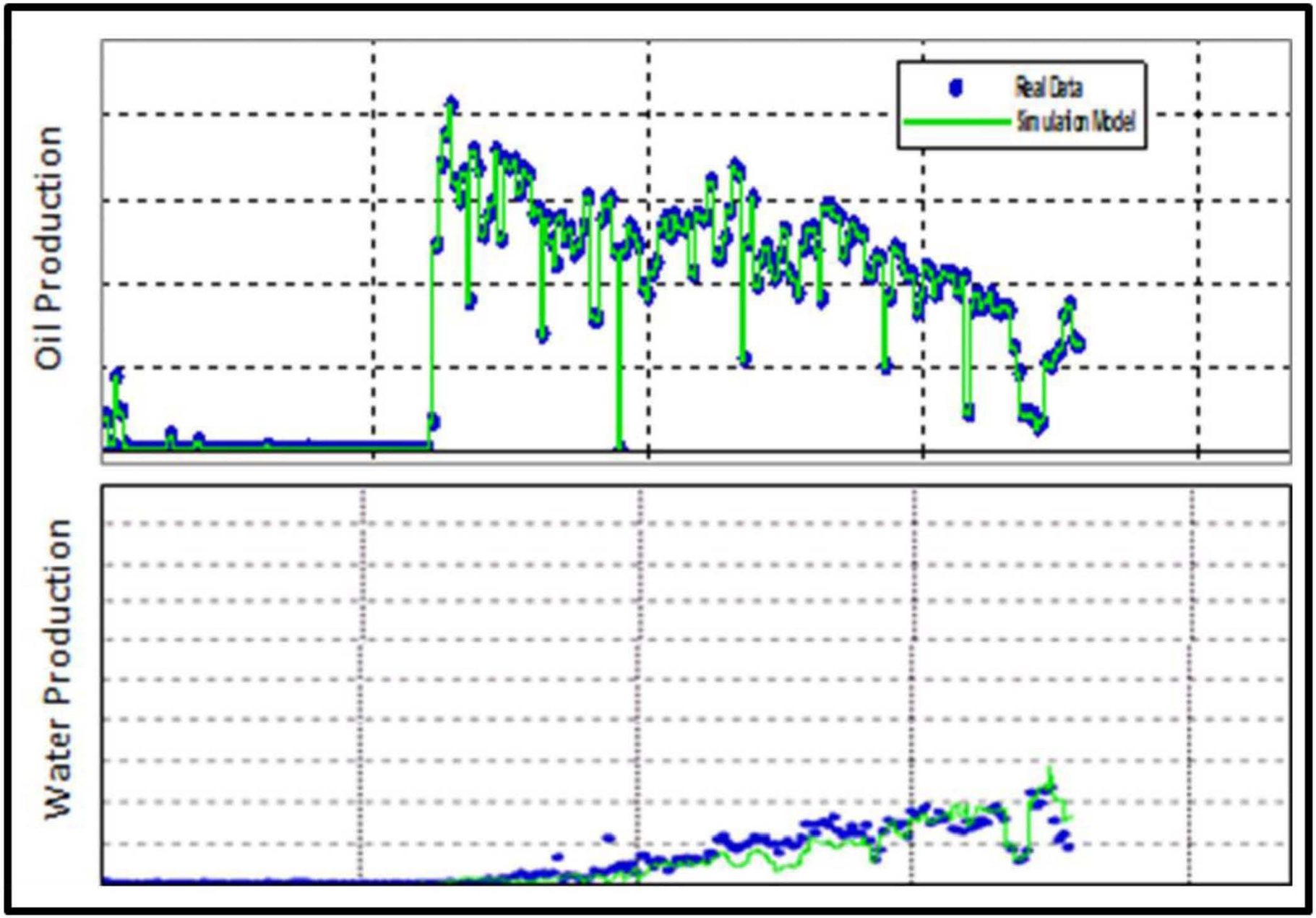

Figure 20. Full-field history match.

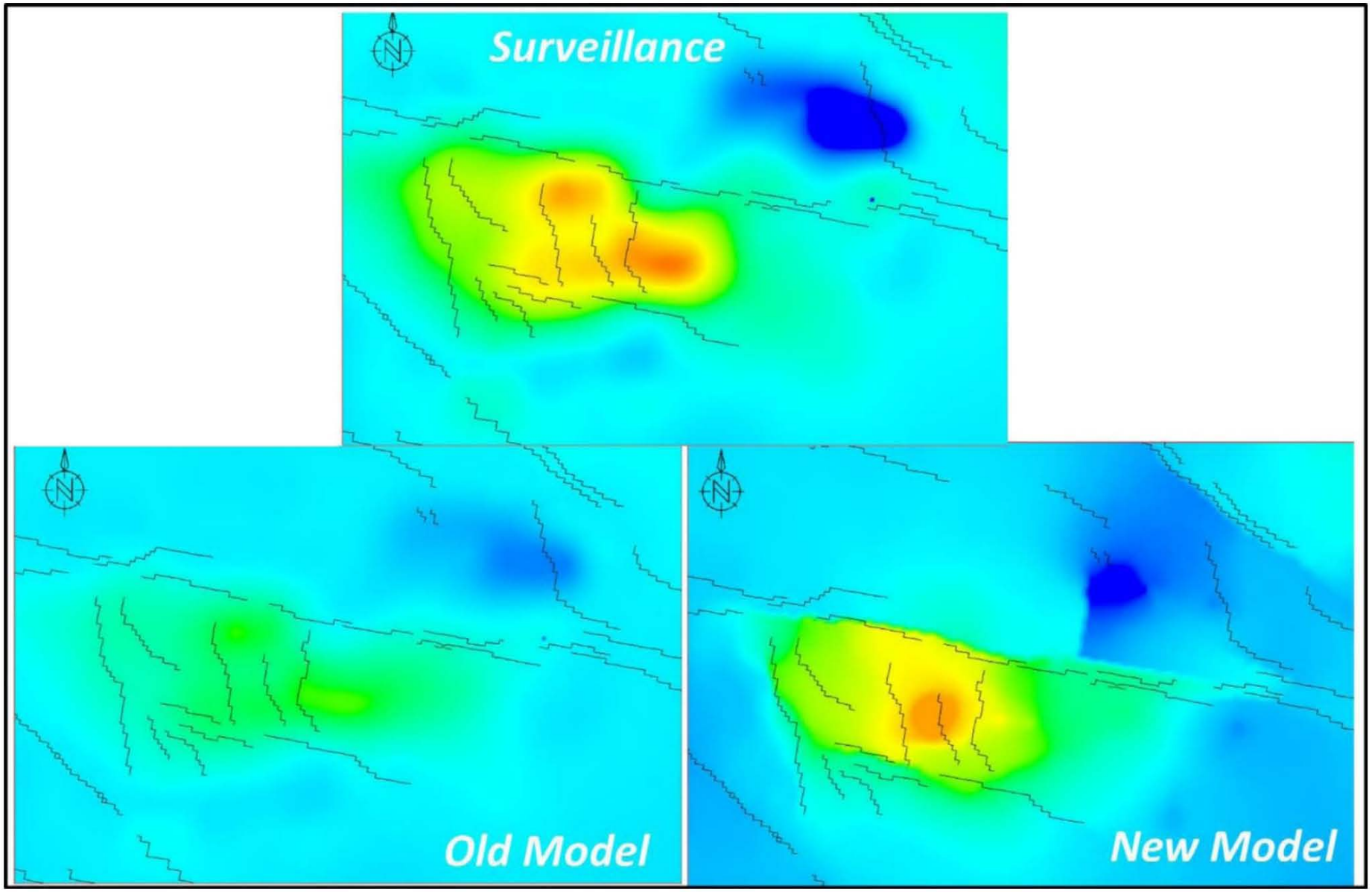

Figure 21. Reservoir pressure map (top: surveillance; left: old model; right: new model). Pressure from the new model can mimic the surveillance pressure measurement.

Nu	Lithofacies	Texture	Reservoir Characteristics	Common Features	Depositional Environment
1	Algal Foraminifera Echinoid Packstone (AFEP)	Packstone	Low porosity (5-8%) Low matrix permeability (~3mD)	Abundant Algal, Foraminiferas, and Echinoids. Moderate to well sorted Bimodal grain size distribution	Lagoon
2	Algal Skeletal Rudstone (ASR)	Rudstone	Low porosity (~10%) Low matrix permeability (~5mD)	Some Bacinella and abundant bioclasts. Aggregate grains, intraclasts. Poor to moderate sorted Bimodal grain size distribution	Lagoon
3	Bioturbated Skeletal Peloid Packstone (BSPP)	Packstone	Low porosity (~7%) Low matrix permeability (<1mD)	Abundant Peloids and many bioclasts (Bivalves, Gastropods, Foraminiferas, Echinids, Sponge Spiculas). Bioturbation is common. Moderate to well sorted	Lagoon
4	Foraminifera Peloid Wackestone Packstone (FPWP)	Wackestone to Packstone	Low porosity (~7%) Low matrix permeability (3-5mD)	Abundant Foraminiferas, Peloids, Sponge spicules, Algae and Echinids. Moderate to well sorted. Bioturbated	Lagoon
5	Ooids Peloid Skeletal Grainstone (OPSG)	Grainstone	Moderate to high porosity (15%) Permeability is up to 1+D) Interparticle, intraparticle, and microporosity.	Abundant Ooids, Peloids, and Bioclasts. Well sorted.	Shoal Barrier
6	Skeletal Peloid Packstone	Packstone to Grainstone	Moderate to high porosity (15%)	Foraminifera, Echinids, Algae and Bivalves.	Shoal Barrier
	Grainstone (SPPG)		Permeability is up to 1+D) Interparticle, intraparticle, and microporosity.	Peloids are abundant. Sparry calcite cement is present. Well sorted.	
7	Bacinella Oncoid Boundstone (BOB)	Boundstone	Moderate to high porosity (15%) Permeability is up to 1+D) Interparticle, intraparticle, and microporosity.	Centrimetric Bacinella and Oncoids.	Outer Protected Ramp
8	Oncoid Peloid Floatstone Rudstone (OPFR)	Floatstone to Rudstone	Good porosity (~15%) Moderate matrix permeability (5-20mD)	Abundant Onchoids and Peloids. Moderate to well sorted Unimodal to bimodal grain size distribution	Outer Protected Ramp
9	Oncoid Peloid Packstone Floatstone (OPPF)	Packstone to Floatstone	Moderate porosity (10-12%) Moderate matrix permeability (5-25mD)	Common Onchoids and Peloids. Poor to moderate sorted Bimodal grain size distribution	Outer Protected Ramp

Table 1. Studied reservoir characterization and depositional environment.